Differential dopaminergic modulation of spontaneous cortico-subthalamic activity in Parkinson's disease

Abhinav Sharma[1], Diego Vidaurre[23], Jan Vesper, Alfons Schnitzler[1], Esther Florin[1]

[1]*Institute of Clinical Neuroscience and Medical Psychology, Medical Faculty, Heinrich-Heine University Düsseldorf*

[2] *Department of Psychiatry, University of Oxford, Oxford, UK*

[3]. *Department of Clinical Health, Aarhus University, Aarhus, Denmark*

Corresponding Author: Esther Florin and Abhinav Sharma

Key Words: Parkinson's, MEG, Oscillations, Time resolved, Hidden Markov Model, Local field potentials, Whole brain, Spectral connectivity, Dopamine

Abstract

Pathological oscillations are a hallmark of neural activity in Parkinson's disease (PD). Time-averaged analyses are usually employed to study changes in spectral connectivity with and without dopaminergic intervention in PD. This prevents differentiating the pathological vs physiological nature of dynamically evolving oscillatory activity serving multiple functional roles. Using a Hidden Markov Model on combined STN-LFP and whole-brain MEG data from 17 PD patients we discovered three distinct network activity patterns. One network was related to adverse effects of increased dopamine, a second one maintained ON-medication spatio -spectrally selective cortico-STN connectivity and finally, a local STN-STN network emerged which indicated the inability of L-DOPA to modify local basal ganglia activity. Temporally we found that, ON medication, the cortico-STN and the STN-STN network increased in duration whereas the cortico-cortical network occurred less frequently. Our results provide a spectrally diverse and spatially specific understanding of transient network connectivity in PD on a whole brain level, disambiguating temporal and spatial changes of the underlying networks. By providing electrophysiological evidence for the differential effects of L-DOPA intervention in PD, our findings open further avenues for electrical and pharmacological intervention in PD.

1 Introduction

Oscillatory activity serves crucial cognitive roles in the brain (Akam and Kullmann, 2010, 2014), and alterations of oscillatory activity have been linked to neurological and psychiatric diseases (Schnitzler and Gross, 2005). Different large scale brain networks operate with their own oscillatory fingerprint and carry out specific functions (Keitel and Gross, 2016; Mellem *et al.*, 2017; Vidaurre, Hunt, *et al.*, 2018). Although such large scale networks remain relatively preserved across humans, there is variability across individuals under both resting conditions and tasks (Mueller *et al.*, 2013; Tavor *et al.*, 2016). Given the dynamics of cognition, different brain networks need to be recruited and deployed flexibly. Hence, the duration for which a network is active, its overall temporal presence and even the interval between the different activations of a specific network might provide a unique window for

understanding brain functions. Crucially, alterations of these temporal properties and / or networks might relate to neurological disorders.

In Parkinson's disease (PD) beta oscillations within the STN and motor cortex (13-30 Hz) are correlated with the motor symptoms of PD (Marreiros *et al.*, 2013; van Wijk *et al.*, 2016; West *et al.*, 2018). At the same time, beta oscillations play a critical role in synchronising communication in a healthy brain (Engel and Fries, 2010). At the cellular level nigral dopamine loss in PD leads to widespread changes in brain networks of varying degrees across patients. Loss in dopamine is managed in patients via dopamine replacement therapy (DRT) (Jubault et al., 2009; Jastrzębowska et al., 2019). Since dopamine is a widespread neuromodulator in the brain (Gershman and Uchida, 2019), this raises the question whether all medication-induced changes can restore physiological oscillatory networks (Voon et al., 2009).

Taking into account both the between-subject and medication-induced heterogeneity, a characterisation of the differential DRT effects has the potential to delineate pathological versus physiologically relevant spectral connectivity in PD. In our present work we studied PD brain activity via a Hidden Markov Model (HMM), a data-driven learning algorithm (Vidaurre et al., 2016; Vidaurre, Hunt, *et al.*, 2018). This allowed us to reveal the temporal properties of connectivity, offering a more complete description of the network activity. Critically, in order to study cortico-subcortical interactions in PD, we recorded combined resting state whole brain MEG and subthalamic nucleus (STN) local field potential (LFPs) from PD patients, and included both modalities into the model. We addressed the effect of DRT on spectral connectivity by acquiring data both OFF and ON medication (L-DOPA).

We found three distinct networks/connectivity profiles that were differentially modulated under medication: cortico-cortical, cortico-STN and STN-STN. Temporally two of the networks preserved selective spectral connectivity ON medication for longer durations. The tendency of neural activity to switch to and revisit the cortico-cortical profile decreased ON medication. Furthermore, the effect of medication was disruptive for the cortico-cortical, physiologically restorative for cortico-STN and relatively benign for the STN-STN profile. These results provide novel information that complete the

oscillatory profiles of network connectivity occurring in PD. This opens up other potential targets for, both electric and pharmacological, interventions in PD.

2 Methods

2.1 Subjects

In total 17 (4 females) right-handed PD patients (age: 55.2 ± 9.3 years) undergoing surgery for therapeutic STN deep brain stimulation (DBS) were recruited for this study. Patients had been selected for DBS treatment according to the guidelines of the German Society for Neurology. The experimental procedure was explained to all participants and they gave written consent. The study was approved by the local ethics committee (study no. 5608R) and conducted in accordance with the Declaration of Helsinki. Bilateral DBS electrodes were implanted in the dorsal part of the STN at the Department of Functional Neurosurgery and Stereotaxy in Düsseldorf. The implanted DBS electrodes used were the St. Jude Medical Directional lead 6172 (Abbott Laboratories, Lake Bluff, USA) and in one case the Boston Scientific Vercise segmented lead (Boston Scientific Corporation, Marlborough, USA).

The DBS leads were externalized and we measured the patients 1 to 3 days after this procedure. In order to simultaneously acquire MEG and LFP signals, we connected the externalised leads to an EEG amplifier integrated with the MEG system. We used a whole-head MEG system with 306 channels (Elekta Vectorview, Elekta Neuromag, Finland) that was housed within a magnetically shielded chamber. All patients were requested to sit still and awake during the data acquisition. To ensure that patients did not fall asleep we tracked patients' pupil diameter with an eye tracker. To remove eye blink and cardiac artefacts, electrooculography (EOG) and electrocardiography (ECG) were recorded along with the LFP and MEG signals. In order to co-register the MEG recording with the individual MRI, four head position indicator (HPI) coils were placed on the patient's head. Their position as well as additional head points were digitized using the Polhemus Isotrack system (Polhemus, Colchester, USA). The data were recorded with a sampling rate of 2400 Hz and a low-pass filter of 800 Hz was applied. An electrode was placed at the mastoid and all LFP signals were referenced to it.

For the clinical OFF medication state, the Parkinson's oral medication was withdrawn overnight for at least 12 hours. In case a patient had an apomorphine pump, this pump was stopped at least 1 hour before the measurement. First, we recorded resting-state activity in the medication OFF state. The patients were then given their morning dose of L-DOPA in the form of fast-acting levodopa. Data were acquired in three runs of 10 minutes, for a total of 30 minutes for each medication condition. We started the ON medication measurement at least half an hour after the administration of the dose and after clinical improvement was seen. The same procedure as for the OFF medication state was followed for the ON medication measurement.

2.2 Pre-processing

All data processing and analyses were performed using Matlab (version R 2016b; Math Works, Natick, USA). Custom-written Matlab scripts and the Brainstorm toolbox (http://neuroimage.usc.edu/brainstorm/Introduction) were used (Tadel *et al.*, 2011). To ensure artefact-free data, two persons independently inspected the data visually, cleaned artefacts, and compared the cleaning output. The cleaned data included changes agreed upon by both the people involved in cleaning. The Neuromag system provides Signal-Space Projection (SSP) vectors for the cleaning of external artefacts from the MEG channels, which were applied. The line noise was removed from all channels with a notch filter at 50, 100, 150, …, 550 and 600 Hz with a 3 dB bandwidth of 1 Hz. The LFP recordings from the DBS electrode were re-referenced against the mean of all LFP-channels. Very noisy and flat MEG/LFP channels were excluded from further analysis. Time segments containing artefacts were removed from the time series. However, if artefacts only regularly occurred in one single channel, this whole channel was removed instead. Frequently arising artefacts following the same basic pattern, as eye blinks or cardiac artefacts, were removed via SSP. All data were high-pass filtered with 1 Hz to remove movement-related low-frequency artefacts. Finally, the data were down-sampled to 1,000 Hz.

Source estimation was performed on these recordings at an individual level using each individual's anatomy. Therefore, using Freesurfer (https://surfer.nmr.mgh.harvard.edu/, v.5.3.0) the individual cortical surfaces were extracted from the individual T1-weighted MRI scans (3 T scanner and 1 mm^3

voxel size). We used the overlapping spheres method with 306 spheres for the forward model. As inverse model we used a Linearly Constrained Minimum Variance (LCMV) beamformer. The data covariance matrix for the LCMV beamformer was computed directly from each 10-minute recording. The data covariance was regularized using the median eigenvalue of the data covariance matrix. The noise covariance was obtained from an empty room recording on the same day as the actual measurement.

2.3 HMM fitting

The Hidden Markov model is a data-driven probabilistic algorithm which finds recurrent network patterns in multivariate time series (Vidaurre et al., 2016; Vidaurre, Abeysuriya, *et al.*, 2018). Each network connectivity pattern is referred to as a "state" in the HMM framework, such that networks can activate or deactivate at various points in time. More specifically, we used a specific variety of the HMM, the time-delay embedded HMM (TDE-HMM), where the states were characterised by spectrally-defined networks at the whole-brain level, defined in terms of both power and phase-coupling (Vidaurre, Hunt, *et al.*, 2018). Hence, for every time point the HMM algorithm provided the probability of a spectrally-defined network being active or "being in a state". This produced a temporally resolved spatial connectivity profile for the underlying time series. In our analysis we also performed spectral analysis of these state visits leading to a complete spatio-spectral and temporal profile of oscillatory activity across the cortex and the subthalamic nucleus. By applying the HMM analysis to the combined MEG-LFP dataset we were able to spatially and spectrally separate cortico-cortical, cortico-STN and STN-STN interactions in time, leading to a more detailed understanding of PD oscillatory activity OFF and ON medication.

2.3.1 Dataset preparation

For each subject the entry point of the STN was identified based on intraoperative microelectrode recordings (Hartmann et al., 2018; Moran et al., 2006; Sterio et al., 2002). Subsequently, the first directional contact present after the entry point was selected to obtain the 3 lfp recordings from the respective hemisphere. This resulted in 3 LFP time series being extracted per brain hemisphere. The source-reconstructed MEG data was projected to the default anatomy (MNI 152 with 15002 vertices)

and then down-sampled temporally to 250 Hz for each medication condition for every subject. We used the Mindboggle atlas to spatially reduce the data dimensions. For every anatomical region (42 cortical regions) in the atlas a multidimensional time series was extracted. The spatial dimensions of this multivariate time series comprised the vertices that were found within an anatomical region as defined by the atlas. Principal component analysis was performed along the spatial dimension, within each region. The resulting first principal component explaining the highest variance in each region was used for the further analysis. The first principal component row vectors from all 42 anatomical regions were stacked into a MEG cortical time series matrix. Subsequently, symmetric orthogonalization (Colclough *et al.*, 2015) was applied to each subject's resulting cortical time series matrix, in order to correct for volume conduction in the signal. The row vectors of this orthogonalized matrix and the 6 LFP data channels (3 for left and right STN each) were standardised. Subsequently they were stacked into one multidimensional time series (N x T) matrix. Here N=48 is the total number of nodes/regions (42 regions from the cortex and 6 LFP electrode contacts) and T denotes the length of the time dimension. This 48 X T data matrix obtained from each subject was concatenated along the temporal dimension across all subjects for each specific medication condition. Finally, in order to resolve sign ambiguity inherent in source-reconstructed MEG data as well as polarity of LFP channels across subjects, a sign-flip correction (Vidaurre *et al.*, 2016) procedure was applied to this final 48 by T by number of subjects dataset within a medication condition.[1]

2.3.2 Estimation of the HMM model

The underlying idea behind a Hidden Markov Model is that the dynamic system can be characterized by a small number of states, each corresponding to a network of activity, and a corresponding transition matrix that captures the probability of the system transitioning between states. Since we were interested in recovering cortico-STN, phase-related communication patterns, the TDE-HMM was fit on the raw time series. This preserved the cross covariance within and across the underlying raw time series of cortical regions and the STN. This information was then exploited by the model to segregate

[1] For details on sign flipping please refer the HMM toolbox wiki: https://github.com/OHBA-analysis/HMM-MAR/wiki/Theory#sign

the data into states. The model estimation finds recurrent patterns of covariance between regions (42 cortical regions and 6 STN contacts) and segregates them into "states". Based on these covariance patterns, for each state the power spectra of each cortical region and the coherence amongst regions can be extracted.

In our model estimation, for the present dataset, 6 states were a reasonable trade-off between spectral quality of results and their redundancy (see supplementary material). The HMM-MAR toolbox (Vidaurre *et al.*, 2016) was used for fitting the TDE-HMM model. We employed the TDE version of the HMM where the embedding took place in a 60 ms window (15 time-points window for a sampling frequency of 250 Hz). Since time-embedding would increase the number of rows of the data from 48 to 48 times the window length (also referred to as No. of lags), an additional PCA (reduction across 48 X No. of lags) step was performed after time embedding. The number of components retained were 96 (48 x 2). This approach follows (Vidaurre, Hunt, *et al.*, 2018). To characterise each Markov state a full covariance matrix was used. We used an Inverse Wishart prior for each covariance matrix. The value of the diagonal of the prior of the transition probability matrix was set as 10. In order to ensure that the mean of the time series does not take part in driving the states the zero mean option in HMM toolbox was set to 1. To speed up the process of fitting we used the stochastic version of variational inference for the HMM. In order to start the optimisation process 'hmmmar' type initialisation was used (for details see (Vidaurre *et al.*, 2016)).

2.4 Statistical analysis of the Markov states

After the six states were obtained for HMM OFF and HMM ON medication, two different kinds of statistical analysis were done.

2.4.1 State comparison across medication conditions

In order to test for differences in coherence the first step was to objectively establish a comparison between the states found in the two HMMs fit separately for each medication condition. There is no a priori reason for the states detected in each condition to resemble each other. In order to find OFF and ON medication states that may resemble each other, we calculated the Riemannian distance (Förstner and Moonen, 2003) between the state covariance matrices of the OFF and ON HMM. This yielded an

OFF states X ON states (6 x 6) distance matrix. Subsequently, finding the appropriately matched OFF and ON states reduced to a standard linear balanced assignment problem. We find an ON state counterpart to each OFF state minimizing the total sum of distances using the Munkres linear assignment algorithm (Vidaurre, Abeysuriya, *et al.*, 2018). This approach yielded a one-on-one pairing of OFF and ON medication states and all further analysis was conducted on these pairs. For ease of reading, we give each pair its own label. For example, when we refer to a "communication" state in the following sections, then such a state was discovered OFF medication and its corresponding state ON medication is its distance-matched partner. Within every result, all mentions of ON or OFF medication refers to these state pairs unless mentioned otherwise.

2.4.2 Intra medication analysis (IntraMed)

We investigated the spectral connectivity patterns across the different states within a medication condition. The objective was to uncover significant coherent connectivity standing out from the background within each spectral band (delta/theta, alpha, beta) in the respective states. The HMM output included the state time courses (i.e. when the states activate) for the entire concatenated data time series. The state time courses allowed the extraction of state- and subject-specific data for further state- and subject-level analysis. For each HMM state we filtered the state-specific data[2] for all the subjects between 1 and 45 Hz to restrict our analysis up to the beta frequency range (13-30 Hz). Then we calculated the Fourier transform of the data using a multitaper approach in order to extract the frequency components from the short segments of each state visit[3]. 7 Slepian tapers with a time bandwidth product of 4 were used, resulting in a frequency resolution of 0.5Hz and therefore binned frequency domain values. Subsequently, we calculated the coherence and power spectral density of this binned (frequency bins obtained during the multitaper step) data for every subject and every state. The coherence and the power spectral density obtained are 3 dimensional matrices of size f (no. of frequency bins) times N (42 cortical locations + 6 STN contacts) times N.

[2] For state-wise data extraction please refer the HMM toolbox wiki (https://github.com/OHBA-analysis/HMM-MAR/wiki/User-Guide).

[3] see (Vidaurre, Hunt, *et al.*, 2018) for discussion on multitaper for short time data segments.

Based on the coherence matrices, we performed a spectral band-specific analysis. Canonical definitions of frequency bands assign equal weight to each frequency bin within a band for every subject. This might not hold true when considering analysis of brain signals across a large dataset. For example, the beta peak varies between individual subjects. Assigning the same weight to each bin in the beta range might wash out the beta effect at the group level. In order to allow for inter subject variability in each frequency bin's contribution to a spectral band, we determined the spectral factors (bands) in a data-driven manner. Because we focused on interactions that are important to establish the STN-cortex communication, the identification of the relevant spectral bands was restricted to the cross-coherence between the STN-LFPs and cortical signals, i.e. the block matrix consisting of rows 1 to 6 (STN) and columns 7 to 48 (cortex). For each subject, this extracted submatrix was then vectorised across columns. This gave us a (No. of frequency bins by 252 [6 STN locations x 42 cortical locations]) matrix for each state. For every subject this matrix was concatenated along the spatial dimension across all states producing a (No. of frequency bins by [252 times 6 (No. of states)]) matrix. We called this the subject-level coherence matrix. We averaged these matrices across all subjects along the spectral dimension (No. of frequency bins) to yield a (No. of frequency bins X [252 * 6]) group-level coherence matrix. In order to obtain the data-driven spectral bands we factorised the group-level coherence matrix using Non Negative Matrix Factorisation (NNMF) (Lee and Seung, 2001). We chose to obtain four spectral bands using NNMF. Subsequently the four spectral bands/components obtained were each of dimensionality equal to the number of frequency bins. Three of them resembled the canonical delta/theta (delta and theta frequencies were combined into one band), alpha, and beta bands whereas the last one represented noise. Since NNMF does not guarantee a unique solution, we performed multiple instances of the factorisation to yield spectral factors that were most frequency specific and stable.

We then projected, i.e. inner product, the subject- and group-level coherence matrix onto the spectral bands obtained above. We called these the subject-level and group-level projection results, respectively.

In order to separate background noise from strongest coherent connections in the projections obtained above, a Gaussian Mixture Model (GMM) approach was used (Vidaurre, Hunt, *et al.*, 2018). For the group-level projection results, we normalized the activity in each state for each frequency band by subtracting the mean coherence within each frequency band across all states. To initialise (selecting priors of the distribution) the mixture model we used two single-dimensional Gaussian distributions with unit variance: One mixture component to capture noise and the other to capture the significant connections. This GMM with two mixtures was applied to coherence values (absolute value) from each state. Connections were considered significant at a p-value of 0.05 (t-statistic) corrected for multiple comparisons (p-val/ [total no. of possible connections in the coherence matrix]).

2.4.3 Inter medication analysis (InterMed)

We used the subject-level projection results obtained above (obtained during IntraMed analysis) to perform InterMed analysis. For a pair of matched states obtained (see State pairs), we performed two-sided independent sample t-tests to compare coherence calculated between different regions of interest (see Dataset preparation). We grouped individual atlas regions together into canonical cortical regions like frontal, sensorimotor, parietal, visual, medial PFC, and STN contacts. For example, in the beta band STN(contacts)-sensorimotor coherence in the OFF condition is compared to the STN(contacts)-sensorimotor coherence in the ON condition. The p-values obtained were corrected for multiple comparisons for a total number of possible combinations.

2.5 Temporal properties of HMM states

To test for changes in the temporal properties OFF vs ON medication we compared the lifetimes, interval between visits, and fractional occupancy for each state both within and across HMMs using two sided independent sample t-tests. Lifetime/dwell time of a state refers to the time spent by the neural activity in that state. Interval of visit is defined as the time between successive visits of the same state. Finally, the fractional occupancy(FO) of a state is defined as the fraction of time spent in each state. In order to restrict extremely short state visits, that might not reflect neural processes, we only used values that were greater than 100 ms within the results for lifetime comparisons.

3 Results

Under resting state conditions in PD patients we simultaneously recorded whole brain MEG activity with local field potentials (LFPs) from the subthalamic nucleus (STN) using directional electrodes implanted for deep brain stimulation (DBS). Using a Hidden Markov Model (HMM) we identified recurrent patterns of transient network connectivity between the cortex and the subthalamic nucleus which we henceforth refer to as an "HMM state". Each HMM state was defined by the spectral coherence calculated between a different pair of regions. Additionally, the time evolution of the HMM states was determined. The PD data was acquired under medication (L-DOPA) OFF and ON conditions, which allowed us to delineate the physiological vs pathological spatio-spectral and temporal changes observed in PD.

3.1 Spontaneous resting-state PD activity can be resolved into distinct states

Motor network based studies have (Boon *et al.*, 2019) evaluated specific cortico-subthalamic spectral interactions but did not judiciously factor the whole brain changes affecting them. On the other hand resting state whole brain MEG studies identified network changes related to both motor and non-motor symptoms of PD (Olde Dubbelink, Stoffers, Deijen, Twisk, Stam and Berendse, 2013; Olde Dubbelink, Stoffers, Deijen, Twisk, Stam, Hillebrand, *et al.*, 2013), thus making the findings difficult to disambiguate. Using an HMM we delineated cortico-subthalamic spectral changes from both global source level cortical interactions as well as local STN-STN interactions. From the 6 states of the HMM 3 states could be attributed to physiological meaningful connectivity patterns. The other 3 states did not show clear spectral patterns and were therefore not considered in the following (see supplementary figures S1-S3). Figures 2-4 show the connectivity patterns and power variations for the three physiologically meaningful states in both the OFF (top row) and ON medication condition (bottom row). The connectivity was visualised for the spectral bands shown in Figure 1. We refer to the state obtained in Figure 2 as the *hyper-dopaminergic state (hyperDA)*. The frontal cortex changes observed in this state, ON medication, were in line with the dopamine overdose hypothesis (Kelly *et al.*, 2009; MacDonald and Monchi, 2011), hence this state was labelled as hyper-DA. This state was characterised mostly by local coherence within segregated networks OFF medication. In contrast, ON medication

there was a widespread increase in coherence across the brain and loss in specificity of connections. Figure 3 displays the second state that we denote as the *communication state (comms)*. A large proportion of spectral connections in this state enable cortico-STN communication (Lalo *et al.*, 2008; Litvak *et al.*, 2011; Hirschmann *et al.*, 2013; Oswal *et al.*, 2016; van Wijk *et al.*, 2016), thus we labelled this as the communication state. This state was characterised by increased interactions between the STN and the cortex OFF medication, with increased specificity of cortical-STN connectivity ON medication. Finally, Figure 4 shows the third state that we denote as the *local state (local)*. Within this state STN-STN spectral connectivity, both OFF and ON medication was characterized and we therefore named it the local state. Highly synchronous STN activity emerged in this state. The spectral characteristics of this state largely remain unaffected under the influence of dopaminergic medication. In the following sections we describe these three states in detail.

3.2 Hyper-dopaminergic state is characterised by increased frontal coherence due to elevated dopamine levels

Dopamine replacement therapy (DRT) is known to produce cognitive side effects in PD patients (Voon *et al.*, 2009). According to the dopamine overdose hypothesis a reason for these effects is the presence of excess dopamine in brain regions which are not affected in PD (MacDonald and Monchi, 2011). Previous task based and neuroimaging studies in PD demonstrated indirectly frontal cognitive impairment due to dopaminergic medication (Cools *et al.*, 2002; Ray and Strafella, 2010; Macdonald *et al.*, 2016). Supporting the dopamine overdose hypothesis in PD we identified using the HMM framework, to our knowledge for the first time, a delta/theta oscillatory network involving lateral and medial orbitofrontal cortical regions under resting state conditions.

This network emerged primarily between the lateral and medial orbitofrontal cortex ON medication through an intra medication analysis (p-value < 0.05; corrected for multiple comparisons). On the contrary, OFF medication no significant connectivity was detected in the delta/theta band. In the alpha and beta band OFF medication there was significant connectivity (p-value < 0.05) within the frontal regions, STN, and to a limited extent in the posterior parietal regions. There was sparse inter-cortical and cortico-STN communication. Frontal-STN coherence emerged in the alpha band and sensory (pre

motor cortex) –frontal (cortico-cortical) coherence emerged in the beta band. ON medication was no significant connectivity in the alpha and beta band.

Inter medication analysis revealed significantly increased coherence between frontal cortex-STN and temporal cortex-STN, ON compared to OFF, across all spectral bands (p-value < 0.05). The change in sensorimotor-STN connectivity primarily took place in the alpha band (p-value < 0.001) with an increase ON medication. Bilateral STN coherence remained unchanged OFF vs ON medication across all spectral bands.

Viewed together, the above findings point towards a generic increase in alpha and beta band connectivity ON medication across connections due to which none of the connections were significantly different from the mean level of connectivity. We did not observe any significant cortico-STN interaction in any of the spectral bands ON medication. ON medication significant coherence emerged in the delta/theta band primarily between different regions of the orbitofrontal cortex. Increased frontal cortical coherence in the orbitofrontal cortex points towards an overdosing effect of elevated tonic dopamine levels. The hyper-dopaminergic state also captured the generic widespread coherence increase that occurred across the cortex due to medication. Overall, this state provided electrophysiological evidence in support for the cognitive deficits observed in PD ON medication even under resting state conditions.

3.3 The connectivity in the communication state was selectively reduced by dopaminergic medication

Maintenance of beta and alpha band connectivity between specific cortical regions and the STN is an important effect of DRT in PD (Litvak *et al.*, 2011; Hirschmann *et al.*, 2013; Oswal *et al.*, 2016). Previous MEG-LFP studies were unable to capture simultaneous cortico-cortical as well as STN-STN changes within different frequency bands. Our analysis revealed a state which was characterised by selective cortico-STN spectral connectivity and an overall shift in cortex wide activity towards physiologically relevant network connectivity ON medication.

Intra medication analysis ON medication indicated the role of dopamine in pruning connectivity as well as activating region-specific connectivity. First of all, there was a reduction in the anatomical overlap

between alpha and beta band connectivity, i.e. spectral specificity was increased. Second, the connectivity between STN and cortex became more selective (p-value< 0.05; corrected for multiple comparisons). In the alpha band, connectivity between temporal and parietal cortical regions and the STN remained preserved ON vs OFF medication, consistent with previous findings (Litvak *et al.*, 2011). In the beta band most of the connectivity was cortico-cortical in nature. Coherence between the premotor /motor regions and frontal and parietal regions was enhanced ON vs OFF medication (p-value< 0.01). Only STN-medial orbitofrontal connectivity remained intact in the beta band. Motor and premotor coherence with the STN was no longer significant. Region-specific cortical connectivity in the frontal and parietal regions emerged in both the alpha and beta band. Bilateral STN-STN coherence was present in this state ON medication (p-value< 0.05) across all spectral bands.

OFF medication intra medication analysis revealed significant coherence between cortical regions and STN in the alpha and beta band (p-value< 0.05; corrected for multiple comparisons). The cortical regions included parietal, frontal, visual, sensory motor, and temporal cortex. Although beta band connectivity between motor cortex and STN is characteristic in PD patients, amongst our subjects the connectivity leaned towards the pre-motor (sensory) cortical regions. The delta/theta connectivity was restricted to sparse frontal cortex-STN connectivity OFF medication. Cortico-cortical coherence OFF medication showed connections between fronto-parietal, visuo-parietal, and sensory motor-temporal regions (p-value< 0.05; intra medication analysis). There was limited connectivity within specific cortical regions, i.e. there was no local connectivity within the frontal or parietal or sensory motor regions.

Inter medication analysis of coherence yielded effects of dopaminergic medication described in the Parkinsonian literature (Hammond, Bergman and Brown, 2007; Litvak *et al.*, 2011; Hirschmann *et al.*, 2013; Little *et al.*, 2013; Marinelli *et al.*, 2017). There was a significant reduction of coherence across cortical regions from OFF vs ON medication. The STN-sensorimotor (p-value <0.05 [alpha], p-value <0.02 [beta]), STN-temporal (p-value <0.01 [alpha], p-value <0.05 [beta]) and STN-frontal (p-value <0.01 [alpha], p-value <0.001 [beta]) coherence was significantly decreased ON medication. There was no significant change in bilateral STN coherence between medication conditions. Finally, no significant changes due to medication were found in the delta/theta band.

To summarise, coherence decreased ON medication across a wide range of cortical regions both at the cortico-cortical and cortico-STN level. Still significant connectivity was selectively preserved in a spectrally specific manner ON medication both at the cortico-cortical level and the cortico-STN level. The most surprising aspect of this state was the emergence of bilateral STN-STN coherence ON medication across all spectral bands. The results provide evidence for the plausible role of dopamine to increase the signal to noise ratio across the brain.

3.4 Dopamine does not show a significant effect on alpha/beta oscillations within the local state

STN-STN intra hemispheric oscillations positively correlate to motor symptoms' severity in PD OFF medication, whereas dopamine dependent nonlinear phase relationships exists between interhemispheric STN-STN activity (West *et al.*, 2016). Crucially none of the previous studies could rule out the influence of cortico-STN connectivity on the observed changes. Using our data-driven framework we were able to delineate a state which showed exclusive STN-STN connectivity both OFF and ON medication through the intra medication analysis. Both within each STN and across STNs OFF medication STN-STN connectivity was present across all spectral bands (p-value< 0.05; corrected for multiple comparisons). ON medication, the local STN-STN delta/theta oscillations were no longer significant. Importantly significant cortico-STN interactions that could have effected STN-STN oscillations were captured separately in the communication state mentioned previously.

Inter medication analysis revealed that across the entire cortex inter-cortical and STN-cortico coherence was reduced across the spectrum from OFF to ON medication condition. The most affected areas were similar to the ones in the communication state, i.e. the sensory motor, frontal, and temporal regions. Their coherence with the STN was also significantly reduced across the spectrum (STN-sensorimotor (p-value <0.01 [delta/theta], p-value <0.05 [alpha], p-value <0.01 [beta]), STN-temporal (p-value <0.01 [delta/theta], p-value <0.01 [alpha], p-value <0.01 [beta]) and STN-frontal p-value < 0.01[delta/theta], p-value < 0.01 [alpha]), p-value <0.01 [beta]). However, bilateral coherence between STNs was not significantly different in any of the spectral bands.

In summary, inter medication analysis revealed that, in the local state, coherence decreased from OFF to ON medication at both the cortico-cortical and the cortico-STN level. Despite this decrease, intra medication analysis revealed that none of the cortico-cortical or the cortico-STN connections were significantly different from the mean level of connectivity in either medication condition. Furthermore, STN-STN connectivity was not significantly altered OFF to ON medication. Yet intra medication analysis revealed that this STN-STN activity was significantly different from the mean level of connectivity within both medication conditions in the alpha and beta band. This potentially points towards the limited ability of tonic dopamine to modify local STN connectivity in PD.

3.5 Longer lifetimes were observed for states showing a generic decrease in coherence ON medication

So far, we had identified three distinct HMM states, which were differentially modified, both spatially and spectrally, under the effect of dopaminergic medication. Previous research has shown that, ON medication, spectrally specific cortico-STN connectivity remains preserved in PD (Litvak *et al.*, 2011; Hirschmann *et al.*, 2013) which indicates the existence of functionally relevant cortico-STN loops. Also a decrease in coherence between the cortex and the STN has been observed ON medication (George *et al.*, 2013a) which is correlated with improved motor functions in PD. Using the temporal properties available through the HMM analysis we wanted to resolve whether our determined states are of pathological or physiological nature. A state, which is most likely of physiological nature, would have increased lifetime and/or would occur more often ON medication.

OFF medication the local state was the one with the longest lifetime (lifetime local > hyperDA; p-value < 0.01, local > comms p-value < 0.01; corrected for multiple comparisons). The communication state, OFF medication, had the shortest lifetime among all states (comms < hyperDA; p-value <0.01) and the shortest interval between visits (interval of visit comms < hyperDA; p-value < 0.01, comms < comms p-value < 0.01). The largest interval was for the hyper-dopaminergic state OFF medication (hyperDA > local; p-value < 0.01, hyperDA > comms; p-value < 0.01). The fractional occupancy (FO) for the local and communication state was similar, but significantly higher than for the hyper-dopaminergic state (local > hyper-DA; p-value < 0.01, local ~= comms; p-value=0.65, comms > hyperDA; p-value <0.01). ON medication the relative temporal properties of all three states retained the same ordering as for OFF

medication. However, the lifetime of the communication state was no longer significantly different from that of hyper-dopaminergic state.

The lifetimes for both the local and communication state were significantly increased with medication (ON >OFF; local, p-value<0.01); comms, p-value=<0.01) but that for the hyper-dopaminergic state was not influenced by medication. The hyper-dopaminergic state was visited even less often ON medication (Interval on > off hyperDA; p-value<0.01). The interval between visits remained unchanged for the local and communication states. The FO for all three states was not significantly changed from OFF to ON medication. According to the temporal properties analysed, the hyper-dopaminergic state was visited least often compared to the other two states both OFF and ON medication

Under resting state conditions, the local state, showing limited spectral modulation due to dopaminergic medication, lasted the longest. It is possible that under relevant task conditions the communication state that tends to show larger functional specialisation in spectral connectivity, might outlast all others or occur most often.

4 Discussion

In this study we parsed simultaneously recorded MEG-STN LFP signals into discrete time-resolved states in order to reveal distinct spectral communication patterns. Thereby we identified three states in both medication conditions showing distinct coherence patterns. We classified them as hyper-dopaminergic, communication, and local state. Overall, our results indicate a general tendency of neural activity to engage in connectivity patterns in which coherence decreases under the effect of dopaminergic medication and which maintain selective cortico-STN connectivity (communication and local states). Only within the hyper-dopaminergic state coherence increased under dopaminergic medication. These results are in line with multiple effects of dopaminergic medication reported in resting and task based PD studies (Jubault *et al.*, 2009; West *et al.*, 2016; Tinkhauser *et al.*, 2017). Moreover, the differential effect of dopamine allowed us to delineate pathological and physiological spectral profiles.

The hyper-DA state provides electrophysiological evidence in the delta/theta band for the overdose effect of dopaminergic medication in PD. Prior to this there was only indirect anatomical evidence

through task based studies or neuroimaging based results (Cools *et al.*, 2002; Ray and Strafella, 2010; Macdonald *et al.*, 2016). The communication state revealed a complete picture of both cortico-cortical and STN-STN interactions that emerge simultaneously with the spectrally and spatially specific cortico-STN interactions that was largely missing in previous studies. The local state revealed the limited ability of dopaminergic medication to modify specifically local STN-STN alpha and beta oscillations. The temporal properties of the states revealed that not only spatio-spectral properties are modified but the overall time as well as number of occurrences of a state are altered. This insight might prove important for modifying medication as well DBS based strategies for therapeutic purposes.

4.1 Increased tonic dopamine causes excess frontal cortical activity

The hyper-dopaminergic state showed significant coherent connectivity between the orbitofrontal cortical regions in the delta/theta band ON medication. According to the dopamine overdose hypothesis (Cools, 2001; Kelly *et al.*, 2009; MacDonald and Monchi, 2011; Vaillancourt *et al.*, 2013) in PD, with dopaminergic treatment the ventral striatal –fronto cortical circuits experience an excessive increase in tonic dopamine levels. This medication-induced increase is due to excessive compensation of dopamine in the ventral striatal circuitry, which experiences a lower loss of dopamine than its dorsal counterpart. The reason is that in PD dopaminergic neurons in the substantia nigra are primarily lost and therefore the dopamine depletion within the dorsal circuity is higher than the ventral (Kelly *et al.*, 2009; MacDonald and Monchi, 2011). Frontal regions involved here include the orbitofrontal cortex, anterior cingulate, and the inferior temporal cortex (Cools, 2006; MacDonald and Monchi, 2011). Increased frontal cortex connectivity potentially explains the cognitive deficits observed in PD, especially related to learning probabilistic reward tasks (Shohamy *et al.*, 2005; George *et al.*, 2013b). In our results the emergence of frontal cortico –cortical coherence (between orbitofrontal and medial orbitofrontal regions) specifically in the delta/theta band points towards cognitive deficits due to increased dopamine in PD with dopaminergic medication.

Coherence increased from OFF to ON medication across frontal temporal and sensory motor cortices both at the cortico-cortical level as well as the cortico-STN level for the hyper-dopaminergic state. But the increase in coherence in the alpha and beta band was observed across all connected regions, hence

none of them were differentially expressed within the bands. Overall, the hyper-dopaminergic state showed an increase in significant frontal cortex connectivity in the delta band which plausibly produces cognitive deficits ON medication.

A comparison of temporal properties of the hyper-dopaminergic state OFF vs ON medication revealed that ON medication the life time of this state remained unchanged, but the interval between visits was significantly increased, while the fractional occupancy of this state was significantly reduced. In fact, the FO of this state was the lowest among the three states. The temporal results indicate that the hyper-dopaminergic state is least visited and least preferred. Hence neural activity ON medication isn't dominated by this state but its presence plausibly explains the cognitive side effects observed ON medication in PD.

4.2 Selective spectral connectivity remains preserved with increased dopamine levels

In line with previous research (Litvak *et al.*, 2011; Hirschmann *et al.*, 2013), within the communication state selective spectral connectivity between the cortex and STN was maintained ON medication. Moreover, local coherent ensembles emerged primarily in the alpha and beta band within frontal and parietal regions. This is in line with previous results obtained for healthy subjects where anterior and posterior cognitive networks were also found using a HMM approach (Vidaurre, Hunt, *et al.*, 2018).

An interesting feature of the communication state was the emergence of local STN-STN coherence in all three spectral bands. It is important to remember that the bilateral STN-STN coherence in the alpha and beta band did not change in the communication state ON vs OFF medication as revealed by inter medication analysis. Only ON medication (Intra medication analysis) this activity became significantly different from mean level of coherence. Since synchrony limits information transfer (Cruz *et al.*, 2009; Cagnan, Duff and Brown, 2015; Holt *et al.*, 2019), it is possible that these local oscillations are a mechanism to prevent excessive communication with the cortex. Another possibility is that a loss of cortical afferents causes local basal ganglia oscillations to become more pronounced. The causal nature of the interaction is an endeavour for future research.

A comparison of temporal properties of the communication state OFF vs ON medication revealed that ON medication the life time of this state significantly increased, but the interval between visits as well as the fractional occupancy remained unaltered. Thus, the temporal properties revealed that neural activity, ON medication, remained longer in the communication state, which was characterised by preserving selective spectral connectivity. The finding is in line with our hypothesis where a connectivity pattern showing physiologically relevant spectral connectivity has a higher probability of occupation ON medication.

4.3 Tonic dopamine has limited effect on local STN-STN interactions

The local STN-STN coherence emerging in the local state was different from the communication state. In the communication state STN-STN coherence accompanied network changes affecting cortico-STN communication ON medication, thereby plausibly fulfilling a functional role. In contrast, in the local state STN-STN coherence emerged without the presence of any significant cortico-STN coherence either OFF or ON medication. This may indicate the exclusivity of the observed STN-STN activity in the local state to emerge due to local basal ganglia circuitry as well as the inability of tonic dopamine to modify basal ganglia circuit activity. These results provide more evidence that the changes in STN-STN coherence observed in previous studies (Little *et al.*, 2013; Oswal, Brown and Litvak, 2013; Shimamoto *et al.*, 2013) might have been due to cortical interaction affecting STN activity. Future studies should analyse changes occurring within the STN by appropriately taking into account the effect of cortico-basal ganglia activity.

Inter medication analysis of the local state revealed ON medication (as compared to OFF) a widespread decrease in coherence at both cortico-STN and cortico-cortical level, which might indicate a shift towards more physiologically relevant neural activity. This is supported by our result that the probability to occupy the local state increased ON medication.

To the best of our knowledge, we are the first to uncover modulation of STN-STN delta/theta oscillations by L-DOPA. Delta/theta oscillations are known to be involved in tasks involving conflict resolution (Zavala, Zaghloul and Brown, no date; Zavala *et al.*, 2014). But these studies were performed

ON medication. Given that our data were collected under resting conditions it is impossible to discern a functional role for delta/theta oscillations for both the local and the communication state.

4.4 Limitations of the study

In the present study we employed a data-driven approach based on an HMM. In order to find the appropriate model, we had to specify the number of states a priori. We selected the number of states by looking at the STN LFP spectral density profiles. Bayesian theory provides the concept of free energy to enable model selection. One could run different models with varying number of states and choose the one with the highest negative free energy. However, model selection based on free energy often does not yield concrete results (Baker *et al.*, 2014). Another limitation is the use of multivariate Gaussian distributions as observation models. Although it improves the tractability of the HMM inference process it is by construction unable to capture higher order statistics of the data beyond the first two moments. Finally, as with almost any operational data-driven approach, there are some hyperparameters and modelling choices that need to rely on decisions by the researcher.

5 Summary

Using a data-driven machine learning approach we identified three distinct network activity profiles (states) that captured differential spectral connectivity in PD. Our findings uncovered a hyper-dopaminergic state which captured the potentially adverse effects of increased dopamine levels due to dopaminergic medication. Furthermore, a communication state was identified, which ON medication, maintained spatio -spectrally selective cortico-STN connectivity. We also found a local STN-STN coherent state, which pointed towards the inability of L-DOPA to modify local basal ganglia activity. Our findings bring forth a dynamical systems approach for differentiating pathological vs physiologically relevant spectral connectivity in PD. Furthermore, we are able to demonstrate that a dynamical systems level approach is able to uncover differential changes induced by altered levels of a neuromodulator.

6 References

Akam, T. and Kullmann, D. M. (2010) 'Oscillations and Filtering Networks Support Flexible Routing of

Information', *Neuron*, 67(2), pp. 308–320. doi: 10.1016/j.neuron.2010.06.019.

Akam, T. and Kullmann, D. M. (2014) 'Oscillatory multiplexing of population codes for selective communication in the mammalian brain', *Nature Reviews Neuroscience*. Nature Publishing Group, pp. 111–122. doi: 10.1038/nrn3668.

Baker, A. P. *et al.* (2014) 'Fast transient networks in spontaneous human brain activity', *eLife*, 2014(3). doi: 10.7554/eLife.01867.

Boon, L. I. *et al.* (2019) 'A systematic review of MEG-based studies in Parkinson's disease: The motor system and beyond', *Human Brain Mapping*. John Wiley and Sons Inc., 40(9), pp. 2827–2848. doi: 10.1002/hbm.24562.

Cagnan, H., Duff, E. P. and Brown, P. (2015) 'The relative phases of basal ganglia activities dynamically shape effective connectivity in Parkinson's disease', *Brain*, 138(6), pp. 1667–1678. doi: 10.1093/brain/awv093.

Colclough, G. L. *et al.* (2015) 'A symmetric multivariate leakage correction for MEG connectomes', *NeuroImage*. Academic Press, 117, pp. 439–448. doi: 10.1016/J.NEUROIMAGE.2015.03.071.

Cools, R. (2001) 'Enhanced or Impaired Cognitive Function in Parkinson's Disease as a Function of Dopaminergic Medication and Task Demands', *Cerebral Cortex*, 11(12), pp. 1136–1143. doi: 10.1093/cercor/11.12.1136.

Cools, R. *et al.* (2002) *Defining the Neural Mechanisms of Probabilistic Reversal Learning Using Event-Related Functional Magnetic Resonance Imaging*, *Soc Neuroscience*. Available at: www.mrc-cbu.cam.ac.uk/imaging (Accessed: 30 July 2020).

Cools, R. (2006) 'Dopaminergic modulation of cognitive function-implications for L-DOPA treatment in Parkinson's disease', *Neuroscience and Biobehavioral Reviews*. Neurosci Biobehav Rev, pp. 1–23. doi: 10.1016/j.neubiorev.2005.03.024.

Cruz, A. V. *et al.* (2009) 'Effects of Dopamine Depletion on Network Entropy in the External Globus Pallidus', *Journal of Neurophysiology*. American Physiological Society, 102(2), pp. 1092–1102. doi: 10.1152/jn.00344.2009.

Engel, A. K. and Fries, P. (2010) 'Beta-band oscillations—signalling the status quo?', *Current Opinion in Neurobiology*, 20(2), pp. 156–165. doi: 10.1016/j.conb.2010.02.015.

Förstner, W. and Moonen, B. (2003) 'A Metric for Covariance Matrices', in *Geodesy-The Challenge of the 3rd Millennium*. Springer Berlin Heidelberg, pp. 299–309. doi: 10.1007/978-3-662-05296-9_31.

George, J. S. *et al.* (2013a) 'Dopaminergic therapy in Parkinson's disease decreases cortical beta band coherence in the resting state and increases cortical beta band power during executive control', *NeuroImage: Clinical*. Elsevier, 3, pp. 261–270. doi: 10.1016/j.nicl.2013.07.013.

George, J. S. *et al.* (2013b) 'Dopaminergic therapy in Parkinson's disease decreases cortical beta band coherence in the resting state and increases cortical beta band power during executive control', *NeuroImage: Clinical*. Elsevier, 3, pp. 261–270. doi: 10.1016/j.nicl.2013.07.013.

Hammond, C., Bergman, H. and Brown, P. (2007) 'Pathological synchronization in Parkinson's disease: networks, models and treatments', *Trends in Neurosciences*, pp. 357–364. doi: 10.1016/j.tins.2007.05.004.

Hirschmann, J. *et al.* (2013) 'Differential modulation of STN-cortical and cortico-muscular coherence by movement and levodopa in Parkinson's disease', *NeuroImage*, 68, pp. 203–213. doi: 10.1016/j.neuroimage.2012.11.036.

Holt, A. B. *et al.* (2019) 'Neurobiology of Disease Phase-Dependent Suppression of Beta Oscillations in Parkinson's Disease Patients'. doi: 10.1523/JNEUROSCI.1913-18.2018.

Jubault, T. *et al.* (2009) 'L-Dopa Medication in Parkinson's Disease Restores Activity in the Motor Cortico-Striatal Loop but Does Not Modify the Cognitive Network', *PLoS ONE*. Edited by P. L. Gribble. Public Library of Science, 4(7), p. e6154. doi: 10.1371/journal.pone.0006154.

Keitel, A. and Gross, J. (2016) 'Individual Human Brain Areas Can Be Identified from Their Characteristic Spectral Activation Fingerprints', *PLoS Biology*. Public Library of Science, 14(6). doi: 10.1371/journal.pbio.1002498.

Kelly, C. *et al.* (2009) 'L-dopa modulates functional connectivity in striatal cognitive and motor networks: A double-blind placebo-controlled study', *Journal of Neuroscience*. Society for

Neuroscience, 29(22), pp. 7364–7378. doi: 10.1523/JNEUROSCI.0810-09.2009.

Lalo, E. *et al.* (2008) 'Patterns of bidirectional communication between cortex and basal ganglia during movement in patients with Parkinson disease.', *The Journal of neuroscience : the official journal of the Society for Neuroscience*. Society for Neuroscience, 28(12), pp. 3008–16. doi: 10.1523/JNEUROSCI.5295-07.2008.

Lee, D. D. and Seung, H. S. (2001) 'Algorithms for non-negative matrix factorization', in *Advances in Neural Information Processing Systems*.

Little, S. *et al.* (2013) 'Bilateral Functional Connectivity of the Basal Ganglia in Patients with Parkinson's Disease and Its Modulation by Dopaminergic Treatment', *PLoS ONE*, 8(12), p. e82762. doi: 10.1371/journal.pone.0082762.

Litvak, V. *et al.* (2011) 'Resting oscillatory cortico-subthalamic connectivity in patients with Parkinson's disease', *Brain*. Narnia, 134(2), pp. 359–374. doi: 10.1093/brain/awq332.

Macdonald, P. A. *et al.* (2016) 'The effect of dopamine therapy on ventral and dorsal striatum-mediated cognition in Parkinson's disease: support from functional MRI Downloaded from', *A JOURNAL OF NEUROLOGY*. doi: 10.1093/brain/awr075.

MacDonald, P. A. and Monchi, O. (2011) 'Differential Effects of Dopaminergic Therapies on Dorsal and Ventral Striatum in Parkinson's Disease: Implications for Cognitive Function', *Parkinson's Disease*. Hindawi Limited, 2011, pp. 1–18. doi: 10.4061/2011/572743.

Marinelli, L. *et al.* (2017) 'The many facets of motor learning and their relevance for Parkinson's disease', *Clinical Neurophysiology*. Elsevier Ireland Ltd, pp. 1127–1141. doi: 10.1016/j.clinph.2017.03.042.

Marreiros, A. C. *et al.* (2013) 'Basal ganglia-cortical interactions in Parkinsonian patients.', *NeuroImage*. Elsevier, 66, pp. 301–10. doi: 10.1016/j.neuroimage.2012.10.088.

Mellem, M. S. *et al.* (2017) 'Intrinsic frequency biases and profiles across human cortex', *Journal of Neurophysiology*. American Physiological Society, 118(5), pp. 2853–2864. doi: 10.1152/jn.00061.2017.

Mueller, S. *et al.* (2013) 'Individual Variability in Functional Connectivity Architecture of the Human Brain', *Neuron*. Cell Press, 77(3), pp. 586–595. doi: 10.1016/j.neuron.2012.12.028.

Olde Dubbelink, K. T. E., Stoffers, D., Deijen, J. B., Twisk, J. W. R., Stam, C. J. and Berendse, H. W. (2013) 'Cognitive decline in Parkinson's disease is associated with slowing of resting-state brain activity: A longitudinal study', *Neurobiology of Aging*. Elsevier, 34(2), pp. 408–418. doi: 10.1016/j.neurobiolaging.2012.02.029.

Olde Dubbelink, K. T. E., Stoffers, D., Deijen, J. B., Twisk, J. W. R., Stam, C. J., Hillebrand, A., *et al.* (2013) 'Resting-state functional connectivity as a marker of disease progression in Parkinson's disease: A longitudinal MEG study', *NeuroImage: Clinical*. Elsevier, 2(1), pp. 612–619. doi: 10.1016/j.nicl.2013.04.003.

Oswal, A. *et al.* (2016) 'Deep brain stimulation modulates synchrony within spatially and spectrally distinct resting state networks in Parkinson's disease', *Brain*. Oxford University Press, 139(5), pp. 1482–1496. doi: 10.1093/brain/aww048.

Oswal, A., Brown, P. and Litvak, V. (2013) 'Movement related dynamics of subthalmo-cortical alpha connectivity in Parkinson's disease', *NeuroImage*, 70, pp. 132–142. doi: 10.1016/j.neuroimage.2012.12.041.

Ray, N. and Strafella, A. P. (2010) 'Dopamine, reward, and frontostriatal circuitry in impulse control disorders in Parkinson's disease: Insights from functional imaging', *Clinical EEG and Neuroscience*. EEG and Clinical Neuroscience Society (ECNS), pp. 87–93. doi: 10.1177/155005941004100208.

Schnitzler, A. and Gross, J. (2005) 'Normal and pathological oscillatory communication in the brain', *Nature Reviews Neuroscience*. Nature Publishing Group, pp. 285–296. doi: 10.1038/nrn1650.

Shimamoto, S. A. *et al.* (2013) 'Subthalamic nucleus neurons are synchronized to primary motor cortex local field potentials in Parkinson's disease', *Journal of Neuroscience*. Society for Neuroscience, 33(17), pp. 7220–7233. doi: 10.1523/JNEUROSCI.4676-12.2013.

Shohamy, D. *et al.* (2005) 'The role of dopamine in cognitive sequence learning: Evidence from Parkinson's disease', *Behavioural Brain Research*. Elsevier, 156(2), pp. 191–199. doi:

10.1016/j.bbr.2004.05.023.

Tadel, F. *et al.* (no date) 'Brainstorm: a user-friendly application for MEG/EEG analysis', *hindawi.com*. Available at: https://www.hindawi.com/journals/cin/2011/879716/abs/ (Accessed: 6 April 2020).

Tavor, I. *et al.* (2016) 'Task-free MRI predicts individual differences in brain activity during task performance', *Science*. American Association for the Advancement of Science, 352(6282), pp. 216–220. doi: 10.1126/science.aad8127.

Tinkhauser, G. *et al.* (2017) 'Beta burst dynamics in Parkinson's disease OFF and ON dopaminergic medication.', *Brain : a journal of neurology*, 140(11), pp. 2968–2981. doi: 10.1093/brain/awx252.

Vaillancourt, D. E. *et al.* (2013) 'Dopamine overdose hypothesis: Evidence and clinical implications', *Movement Disorders*. NIH Public Access, pp. 1920–1929. doi: 10.1002/mds.25687.

Vidaurre, D. *et al.* (2016) 'Spectrally resolved fast transient brain states in electrophysiological data', *NeuroImage*. Academic Press Inc., 126, pp. 81–95. doi: 10.1016/j.neuroimage.2015.11.047.

Vidaurre, D., Abeysuriya, R., *et al.* (2018) 'Discovering dynamic brain networks from big data in rest and task', *NeuroImage*. Academic Press Inc., pp. 646–656. doi: 10.1016/j.neuroimage.2017.06.077.

Vidaurre, D., Hunt, L. T., *et al.* (2018) 'Spontaneous cortical activity transiently organises into frequency specific phase-coupling networks', *Nature Communications*. Nature Publishing Group, 9(1), pp. 1–13. doi: 10.1038/s41467-018-05316-z.

Voon, V. *et al.* (2009) 'Chronic dopaminergic stimulation in Parkinson's disease: from dyskinesias to impulse control disorders', *The Lancet Neurology*. Elsevier, pp. 1140–1149. doi: 10.1016/S1474-4422(09)70287-X.

West, T. *et al.* (2016) 'The Parkinsonian Subthalamic Network: Measures of Power, Linear, and Non-linear Synchronization and their Relationship to L-DOPA Treatment and OFF State Motor Severity', *Frontiers in Human Neuroscience*. Frontiers Media S. A, 10(OCT2016), p. 517. doi: 10.3389/fnhum.2016.00517.

West, T. O. *et al.* (2018) 'Propagation of beta/gamma rhythms in the cortico-basal ganglia circuits of

the parkinsonian rat', *Journal of Neurophysiology*, 119(5), pp. 1608–1628. doi: 10.1152/jn.00629.2017.

van Wijk, B. C. M. *et al.* (2016) 'Subthalamic nucleus phase-amplitude coupling correlates with motor impairment in Parkinson's disease.', *Clinical neurophysiology : official journal of the International Federation of Clinical Neurophysiology*. Elsevier, 127(4), pp. 2010–9. doi: 10.1016/j.clinph.2016.01.015.

Zavala, B. A. *et al.* (2014) 'Midline frontal cortex low-frequency activity drives subthalamic nucleus oscillations during conflict', *Journal of Neuroscience*. Society for Neuroscience, 34(21), pp. 7322–7333. doi: 10.1523/JNEUROSCI.1169-14.2014.

Zavala, B., Zaghloul, K. and Brown, P. (no date) 'The Subthalamic Nucleus, oscillations and conflict'. doi: 10.1002/mds.26072.

FIGURE DESCRIPTIONS

Figure 1:

Title: Data driven spectral factors derived from the OFF and ON medication condition.

Description: Each plotted shows different spectral factors. The Y-axis represents the weights obtained from the NNMF factorisation and the X-axis represents frequency in Hz. The frequency resolution of the factors obtained is 0.5 Hz. 1A shows the OFF medication spectral factors and 1B shows the same derived separately for the ON medication data.

Figure 2:

Title: Coherence based connectivity for the hyper-dopaminergic state as revealed by intra medication analysis

Description: Each node in the circular graph represents a brain region based on the Mindboggle atlas. The colour code represents a group of regions clustered according to (starting from node number 1) STN contacts (contacts 1,2,3 = right STN and contacts 4,5,6 = left STN), frontal, medial frontal, temporal,

sensory-motor, parietal and visual cortices. Only the significant connections (p-val 0.05; corrected for multiple comparisons) are shown.

Columns represent connectivity for different spectral factors as shown in Figure 1.

2A shows results for OFF medication data and 2B for the ON medication condition. The OFF and ON states were matched as described in Methods (section 2.4.1 State comparisons across medication conditions). Overall the hyper-dopaminergic state was characterized by loss of significant connectivity in the alpha and beta band ON medication and the emergence of medial prefrontal-orbitofrontal connectivity in the delta band.

Figure 3:

Title: Coherence based connectivity for the communication state as revealed by intra medication analysis

Description: Colour code and interpretation of the connectivity graph remains the same as Figure 2. Row and column order remains the same as Figure 2.

The communication state was characterised by preservation of selective cortico-STN connectivity ON medication. The connections preserved were also frequency specific ON medication as compared to the OFF condition.

Figure 4:

Title: Coherence based connectivity for the local state as revealed by intra medication analysis

Description: Colour code and interpretation of the connectivity graph remains the same as Figure 2.

Row and column order as well as interpretation remains the same as Figure 2.

The local state was characterised by preservation of STN-STN coherence in the alpha and beta band OFF vs ON medication. STN-STN theta/delta oscillations were no longer significant ON medication.

Figure 5:

Title: Temporal properties of states

Description: 5A shows the fractional occupancy for the three states for the hyper-dopaminergic (Hyper-DA), communication and the local state. Each point represents the mean for a state and error bar represents standard error. The orange plot is for ON medication data and blue is for OFF medication data.

5B mean interval of visits (in milliseconds) of the three states ON and OFF medication. The statistics plotted and the legend are the same as 5A.

5C shows the lifetime (in milliseconds) for the three states. The statistics plotted and the legend are the same as 5A.

Supplementary figures:

Figure S1-S3:

S1-S3 show the 3 additional states that were found in the OFF and ON HMMs. S1-S3 A show the OFF states along with their state numbers and S1-S3 B show the distance matched ON states.

Spectral Factors

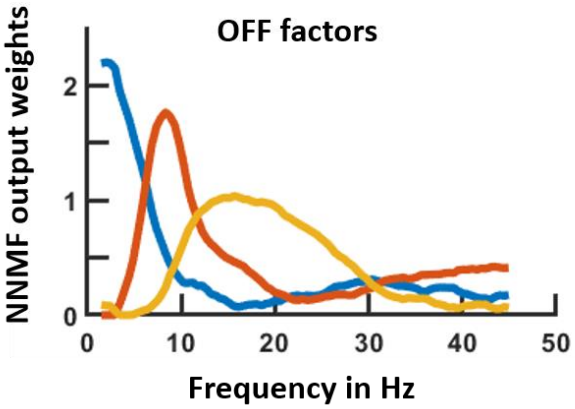

Figure 1A

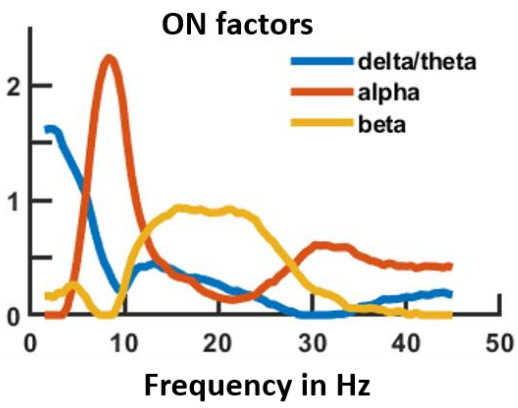

Figure 1B

List of regions in the connectivity ring figures

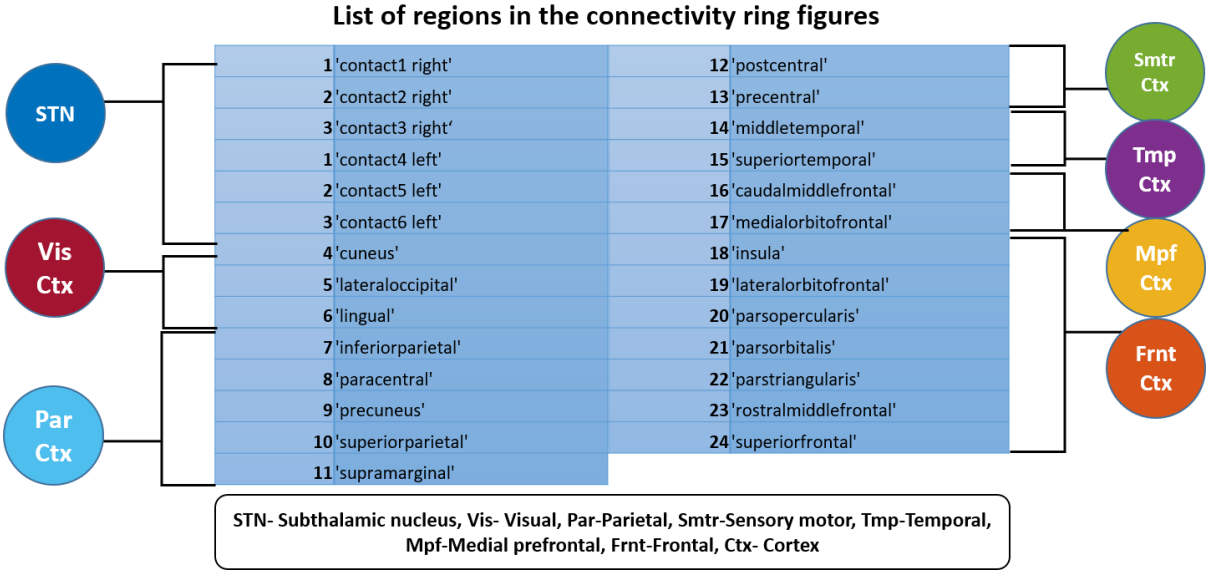

STN- Subthalamic nucleus, Vis- Visual, Par-Parietal, Smtr-Sensory motor, Tmp-Temporal, Mpf-Medial prefrontal, Frnt-Frontal, Ctx- Cortex

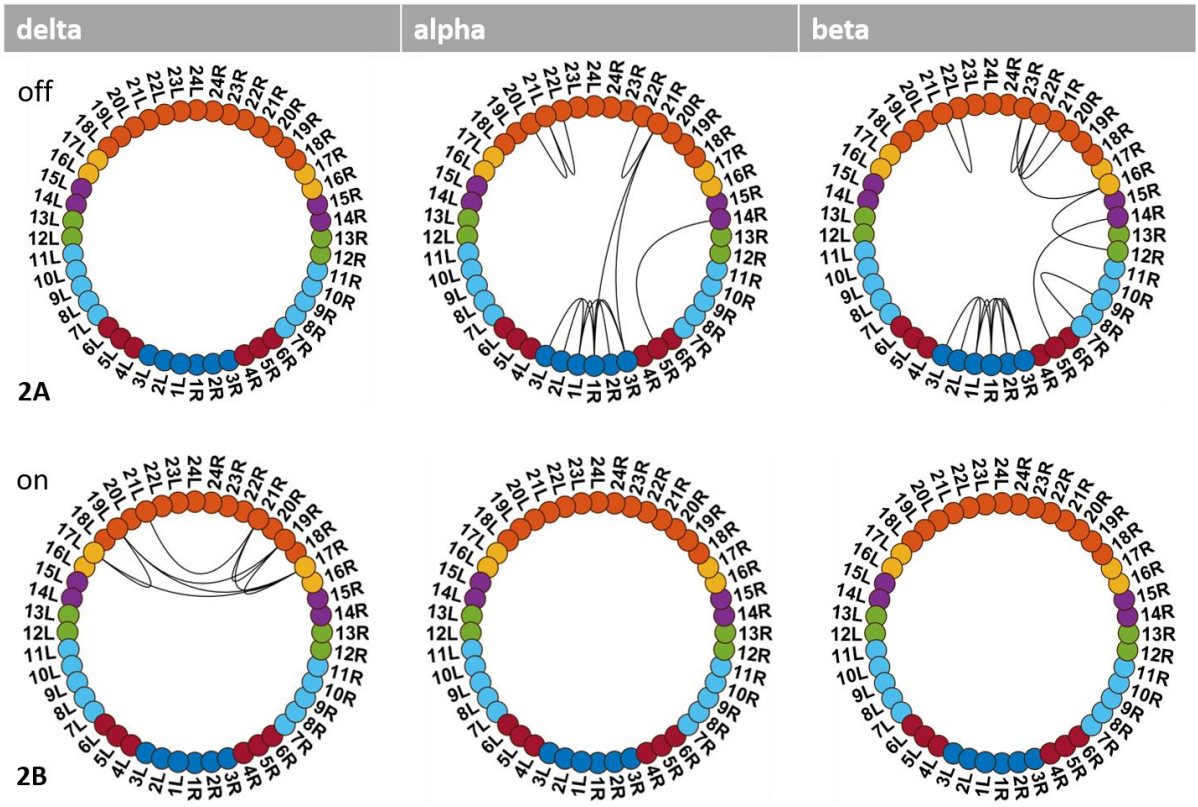

Figure 2: Hyper-dopaminergic state

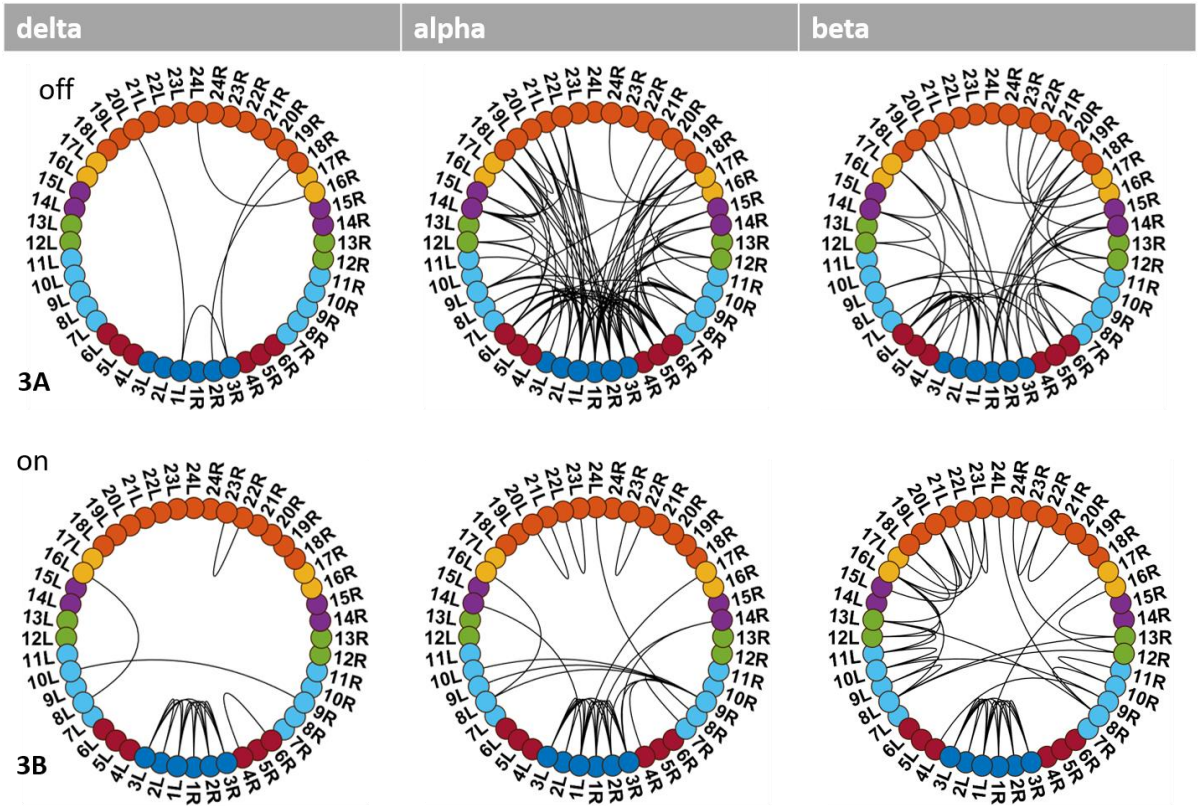

Figure 3: Communication state

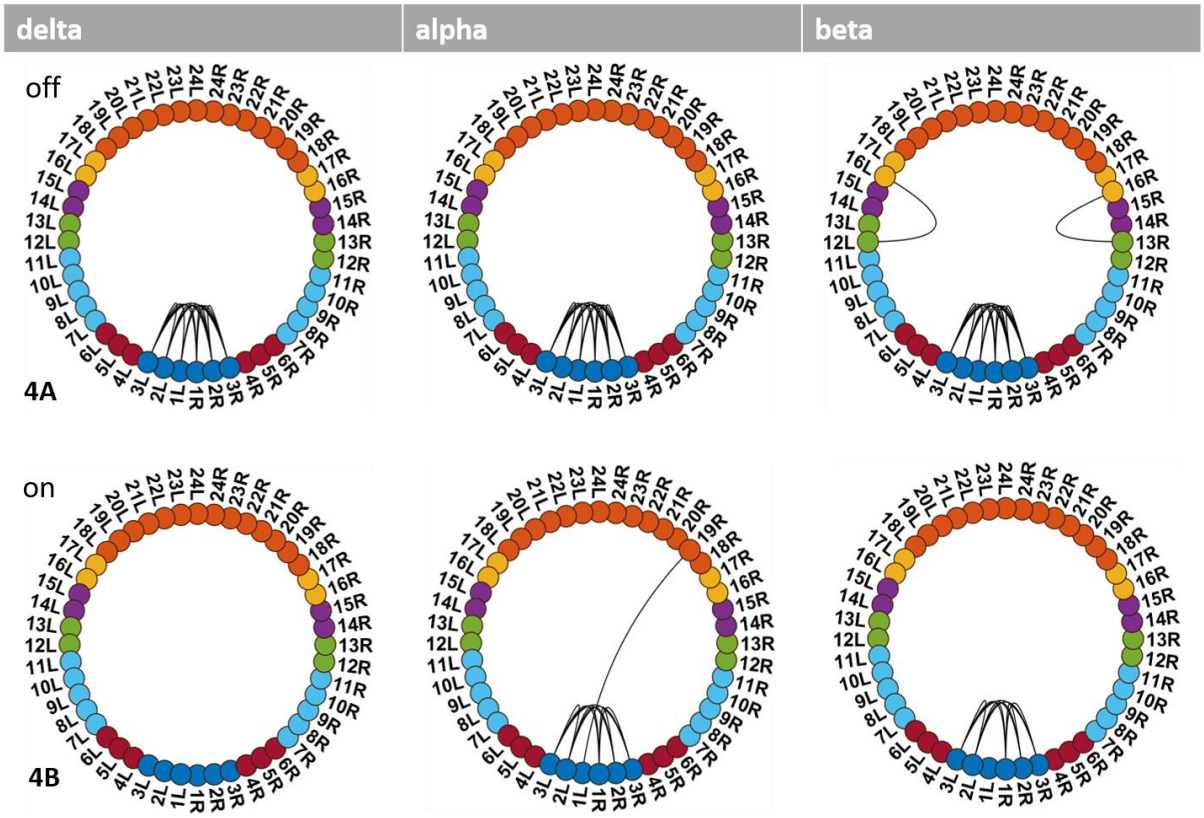

Figure 4: Local state

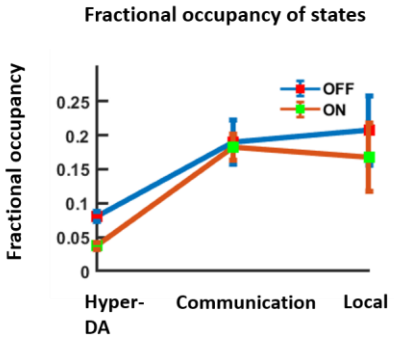

Figure 5A

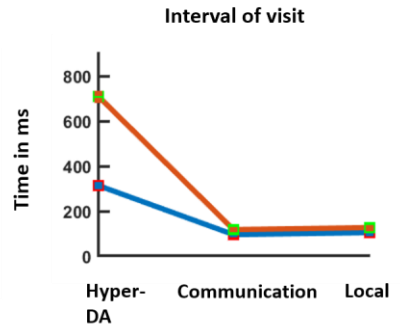

Figure 5B

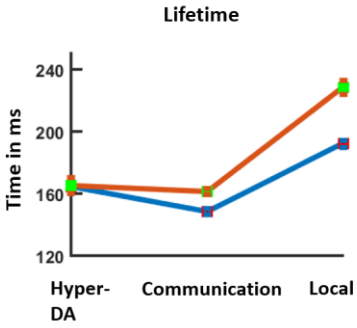

Figure 5C

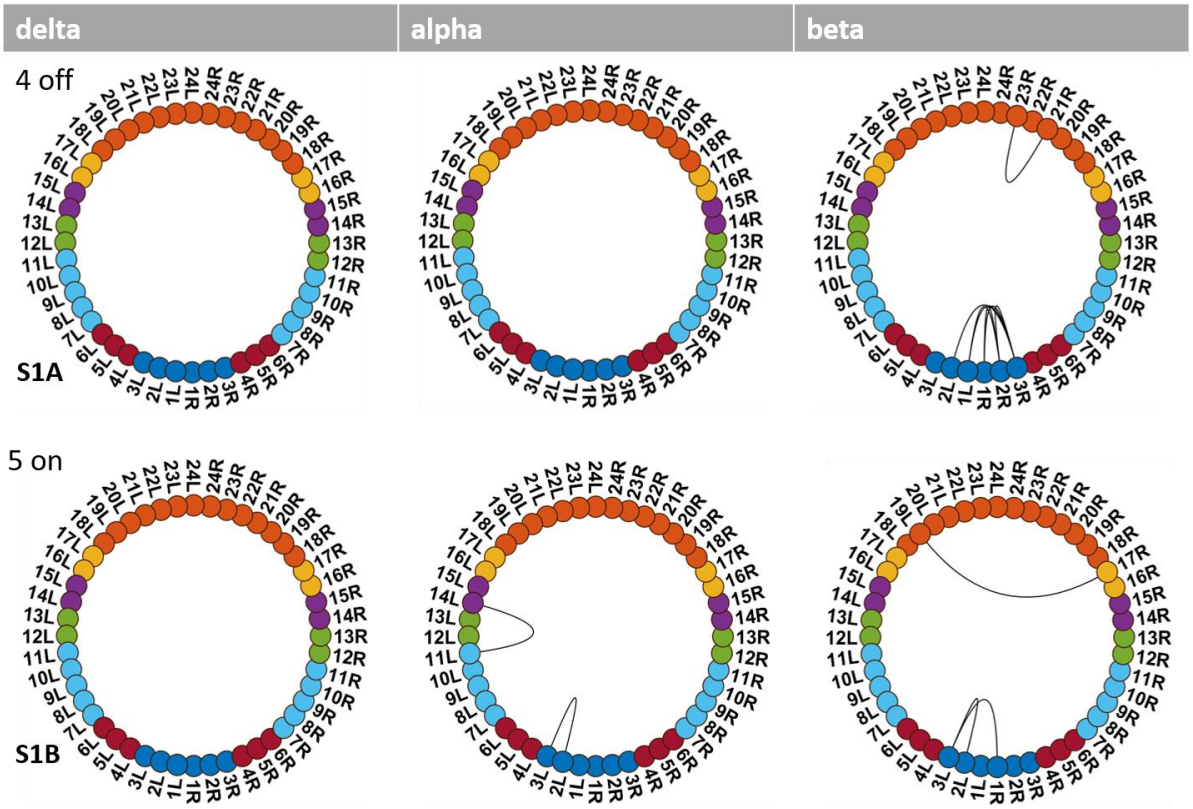

Figure S1: OFF state 4 and ON state 5

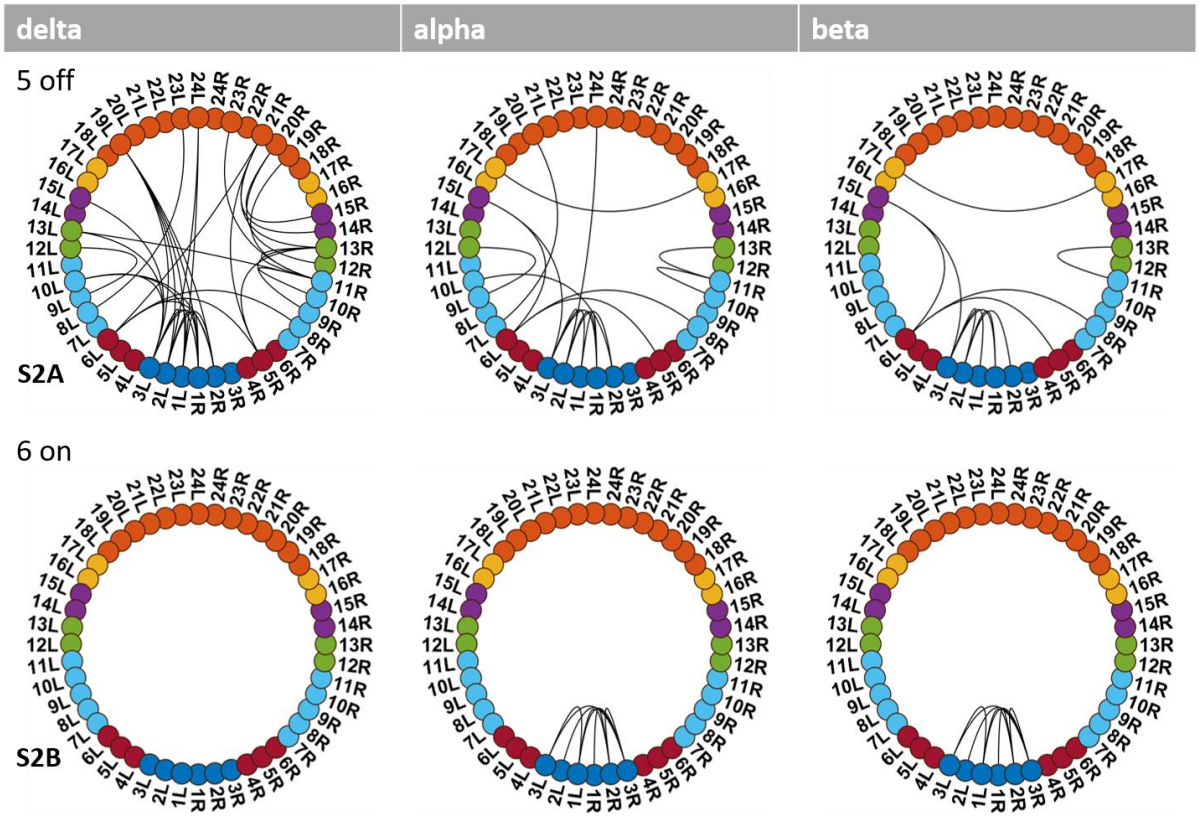

Figure S2: OFF state 5 and ON state 6

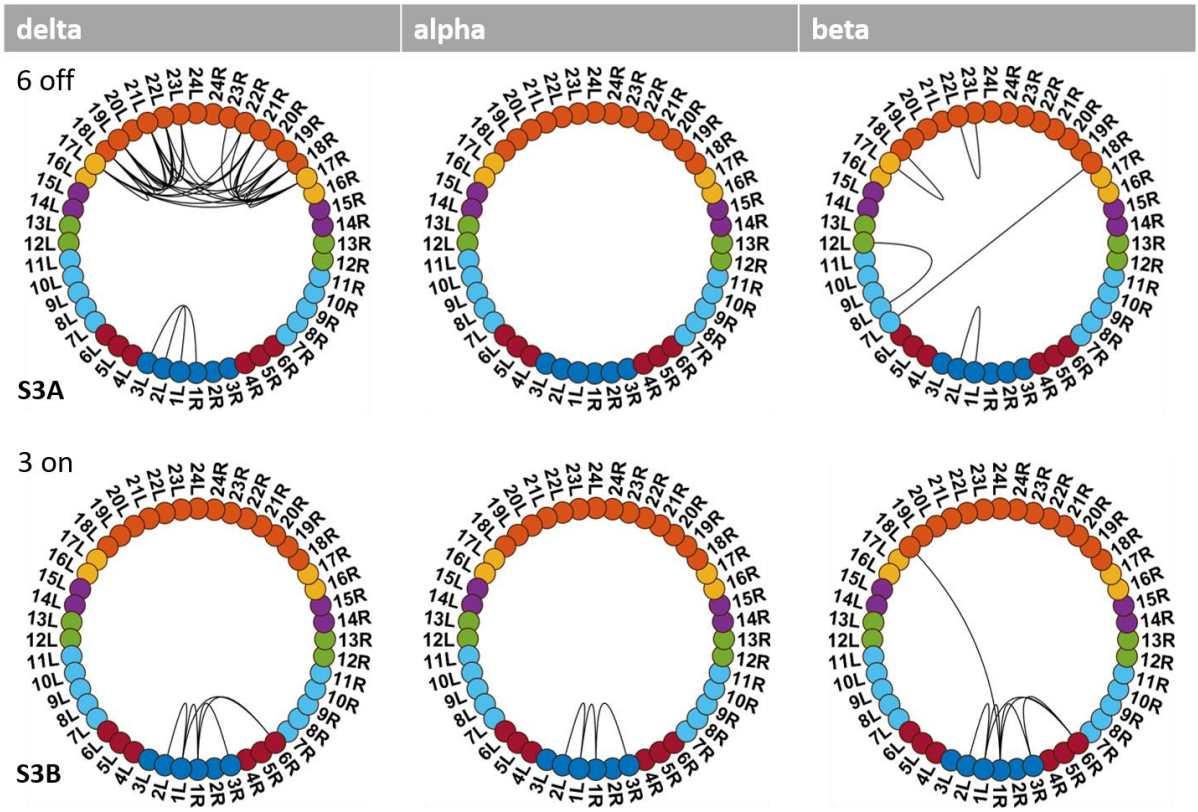

Figure S3: OFF state 6 and ON state 3